

Influence of the intergranular microstructure of substituted nitrides on high temperature strength

J. Y. LAVAL, C. DELAMARRE, M. C. AMAMRA

*Laboratoire de Chimie et Microstructure du Solide Minéral – ERA 912
CNRS-ESPCI, 10, rue Vauquelin – 75231 Paris Cedex 05, France*

D. BROUSSAUD

Centre des Matériaux, Ecole des Mines de Paris B.P. 87 – 91003 Evry Cedex, France

The relationships between the intergranular structure of substituted silicon nitrides and their high temperature strength have been considered. It has been shown that four types of intergranular structure can be distinguished. These structures depend on the nature and amount of additives. Analytical electron microscopy (X-ray microanalysis, micro-diffraction and electron-induced processes) enables a precise characterization of these structures. If an extended glassy phase always appears to be detrimental, it has been shown that a thin glassy film may improve the high temperature strength and the cutting life of sialon tools and may at least be a fair compromise to obtain dense and homogeneous hot-pressed silicon nitrides.

1. Introduction

Silicon nitrides are actively studied for high temperature technology up to 1500°C. This is mainly due to their high thermomechanical and refractory properties and also to their good resistance to corrosion in this temperature range. In order to prepare dense polycrystalline materials, additive oxides are needed as sintering aids. These oxides lead to the formation of secondary phases along grain boundaries. These new phases very often have a glassy structure and greatly modify the mechanical properties of the nitride.

These properties are related to the nature, quantity and distribution of the additive elements in the matrix as well as at the grain boundaries, and also to the firing cycle of the sample. All these factors act on the microstructure. Thus the achievement of given properties implies, as a primary task, the close control of the microstructure.

The microstructure of several types of silicon nitrides are considered and an attempt made to correlate their structure to some mechanical

properties, namely high temperature mechanical strength and cutting efficiency.

2. Experimental methods

This investigation has been carried out by conventional transmission electron microscopy (TEM) and scanning transmission electron microscopy (STEM)

2.1. TEM

High resolution microscopy enables very thin intergranular phases to be located, and electron-induced processes allow the characterization of the non-crystallinity of these phases. Drew and Lewis [1] have pointed out that these glassy phases are selectively attacked by the electron beam. Laval and Westmacott [2] have shown that this process is related to the atomic bonds in the glassy phase. This structure has been confirmed by EXAFS spectroscopy [3]. Such induced atomic processes have a double interest: firstly to show modified bondings with regard to the crystalline structure and secondly to microcharacterize glassy films as thin as 1 nm.

2.2. STEM

To add to this investigation two analytical techniques were applied.

(a) electron microdiffraction: a study of the reciprocal lattice using a very fine beam (spatial resolution $r_s = 20$ nm);

(b) X-ray microanalysis: chemical analysis using a fine electron probe, the spatial resolution ($4 < r_s < 40$ nm) depending on the type of microscope employed.

In order to obtain easily a wide range of information two types of STEM were used. Firstly a Jeol 120 CX with additive scanning attachment and equipped with a silicon-lithium diode for X-ray dispersive energy analysis. The main advantage of this technique is that it can be carried out very easily and concurrently with high resolution electron microscopy ($r_s = 20$ nm in diffraction mode and 40 nm in X-ray mode). However, if one needs to analyse phases smaller than 10 nm, a dedicated STEM (V.G. HB 5) working with a field emission gun (to increase the electron yield) is necessary. The analytical capabilities are then raised up to 3 nm for microdiffraction and 4 nm for X-ray analysis. This technique also provides electron energy loss spectroscopy which leads to complementary chemical analysis on light elements ($Z < 9$) with the best r_s available, i.e. 2 nm. All samples were ion-thinned and carbon-coated by ion-sputtering [4].

3. Description of nitrides

Three varieties of substituted silicon nitrides were studied; a commercial nitride, a well-controlled laboratory nitride, and a commercial sialon.

3.1. Commercial nitride

This material was prepared by hot pressing α - Si_3N_4 powder with 2 wt % MgO as densification aid. The main impurities were found to be iron (0.5%) and calcium (0.25%).

3.2. Laboratory silicon nitride

This nitride was prepared by C. Greskovich [5] from General Electric by hot pressing very fine high purity α - Si_3N_4 powder with an addition of 7 wt % BeSiN_2 . The main impurity consists of oxygen (2.6 wt %) that primarily exists as a surface layer of SiO_2 on Si_3N_4 particles.

This material consists of a single-phase β - Si_3N_4 solid solution of approximate composition $\text{Si}_{2.9}\text{Be}_{0.1}\text{N}_{3.8}\text{O}_{0.2}$ with a density of 99% of theoretical.

TABLE I Composition in major impurities (p.p.m.) for sialons

Element	Sialon A	Sialon B
B	2500	700
C	(1800–18 000)	5000
N		Matrix
O		Matrix
Na	1300	170
Mg	5100	80
Al		Matrix
Si		Matrix
S	140	15
K	140	9
Ca	3600	450
Ti	550	35
V	40	2.5
Cr	150	30
Mn	(60–600)	80
Fe	8000	1100
Ni	45	2

3.3. Commercial sialon

Lucas Industries have proposed, using K.H. Jack's results [6], a pressureless sintering process for yttria sialons (syalons). Due to their excellent mechanical strength and thermal shock resistance and their fairly good fracture toughness, these materials are being developed as tools for metal cutting and are the basis of new improvements in metal machining.

The present investigation was carried out on two different batches (A and B) of Kyon 2000 samples, manufactured by Kenametal USA, which are derived from Lucas Syalon. These two batches resulted in different cutting behaviours. Table I gives the chemical composition of Samples A and B. The contents of Al_2O_3 and Y_2O_3 used as sintering aids for Si_3N_4 were assessed at 6 and 8 wt % respectively for both samples from microprobe analysis. Impurities were analysed by mass spectrometry: Sample A was shown to contain a larger amount of impurities, mainly iron, calcium, magnesium, boron and sodium, than Sample B.

4. Mechanical properties

4.1. Bend strength

The mechanical strength of Si_3N_4 based ceramics varies greatly depending on structural parameters such as residual porosity, average grain size, grain anisotropy (especially for hot-pressed materials) and phase distribution.

The high temperature strength of those ceramics is related to the intergranular structure. The nature of the possible intergranular phase is determined

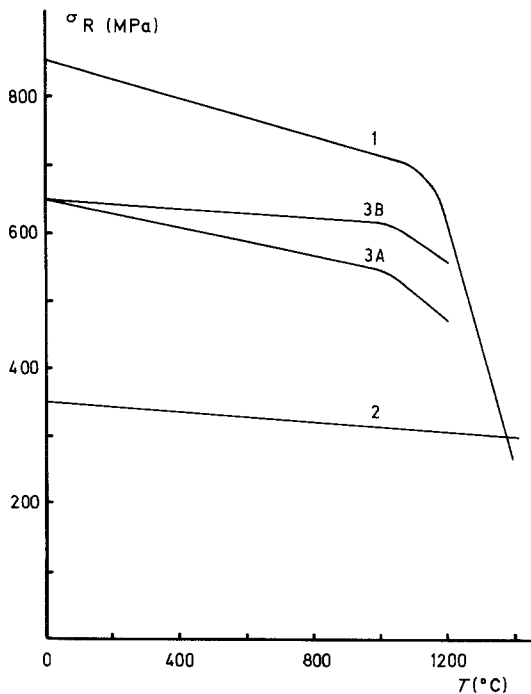


Figure 1 Bend strengths plotted against temperature for the nitrides and sialons studied. 1. Commercial Si_3N_4 (NC 132). 2. Laboratory Si_3N_4 ($\text{Si}_{2.9}\text{Be}_{0.1}\text{N}_{3.8}\text{O}_{0.2}$). 3. Sialons A and B.

by the chemical composition of the sintering additives, impurities and possible reaction with the SiO_2 film found around Si_3N_4 particles. For instance MgO addition is known to yield magnesium silicates likely to melt at fairly low temperature which promotes sintering, but also enhances grain boundary sliding under stress at high temperature. Y_2O_3 addition is then preferred because it gives rise to more refractory phases than MgO .

This consideration explains the strength drop-off observed above 1000°C on commercial nitride and on both sialons, contrary to the laboratory nitride where the strength is reported to be almost constant up to 1400°C . This can be seen in Fig. 1, where bend strengths of the ceramics investigated in this paper are plotted against temperature.

4.2. Cutting behaviour of sialons

The differences in cutting behaviour between sialon batches A and B could not be explained by the simple control of hardness. Both batches were tested [7] for cutting Ni-based superalloy under similar operating conditions (150 mm min^{-1} cutting speed, 0.2 mm min^{-1} feed rate and 5 mm depth of cut). They exhibited different lifetimes: 15 min for Type A samples and only 2 min for Type B samples which failed after showing a rapid evolution of notch wear.

5. Microstructure

In both nitrides the microstructure only reveals a glassy phase at the grain boundaries whereas in the sialons there is a crystalline intergranular phase.

5.1. Nitrides

5.1.1. Commercial nitride

This nitride is shown by TEM to be a highly heterogeneous material as may be seen from the grain size (0.3 to $3\text{ }\mu\text{m}$) as well as from the distribution of the non-crystalline phase. Si_3N_4 grains are embedded in a glassy phase, the size of which is nearly comparable to the matrix (Fig. 2). The intergranular vitreous phase (IVP) can be characterized by electron-induced processes. Under electron irradiation a selective mottled contrast

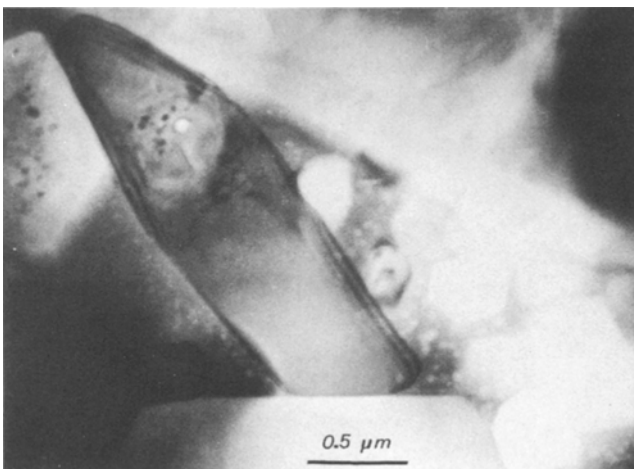


Figure 2 Commercial silicon nitride microstructure.

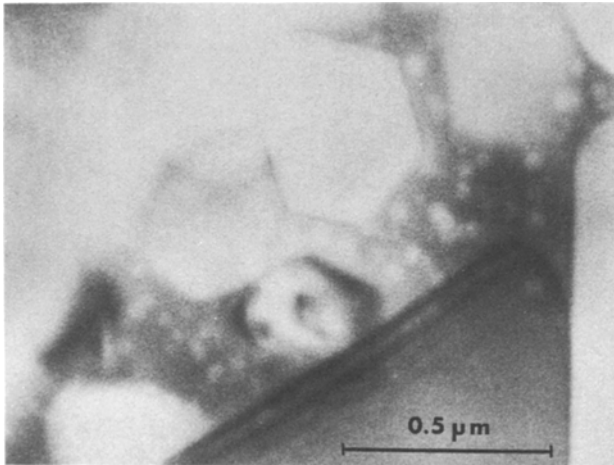


Figure 3 Electron-induced effects on the nitride glassy phase.

corresponding to gas bubble formation may be seen in the glassy phase [2] (Fig. 3). This phenomenon can only be explained by admitting a structural transformation similar to that observed for alkali silica glass [8]. X-ray dispersive energy analysis shows magnesium and calcium enrichment in the IVP, whereas electron energy loss spectroscopy shows oxygen enrichment. Moreover, EXAFS spectroscopy confirms the presence of Si-O⁻ bonds where the O-O spacings can be shorter than in crystalline silica (Fig. 4). Only Si-O⁻ bonds are broken by the electron beam and free oxygen bubbles are formed. The electron-induced processes are governed by irradiation conditions (accelerating voltage and electron beam density) [9].

5.1.2. Laboratory nitride

Contrary to the previous nitride, Si_{2.9}Be_{0.1}N_{3.8}O_{0.2} is a very homogeneous material, with a very regular granulometry (average grain size 0.5 μm) (Fig. 5).

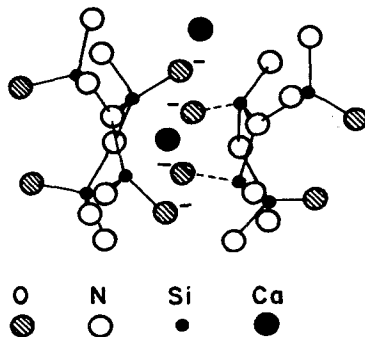


Figure 4 Bonding structure of the glassy phase.

The crystalline structure is β-Si₃N₄ type for the whole sample.

TEM reveals a very fine and regular IVP (1 to 1.5 nm). This thin glassy film is perfectly continuous all along the grain boundaries and does not widen at the triple points, which is remarkable in sintered silicon nitride (Fig. 6).

The composition of the IVP cannot be obtained by chemical microanalysis. Beryllium ($Z = 4$) cannot be detected by X-ray analysis nor by electron energy loss since the Be/ K and Si/ L edges overlap. Moreover the thinness of the IVP impedes any significant analysis of the intergranular silicon, the interaction with the matrix being prohibitive. Thus the only way to be able to assume a beryllium enhancement in the IVP is from induced processes, which can be obtained all along the IVP (Fig. 7). The structural model [9] postulates the segregation of an homovalent cation in the non-crystalline phase which can only be beryllium in this case.

5.2. Sialons

X-ray diffraction on the surface of platelets reveals that the silicon nitride transformation $\alpha \rightarrow \beta$ is more complete for Sample A ($\alpha/\beta = 0.14$) than for Sample B ($\alpha/\beta = 0.25$).

5.2.1. Characterization of an intergranular crystalline phase (ICP)

Samples A and B exhibit a similar granular structure. TEM reveals in both cases (Fig. 8) a very heterogeneous microstructure corresponding to a grain size between 0.1 and 1 μm. The structure is always biphased with a fairly well developed ICP. STEM (Fig. 9) seems to indicate a smaller amount

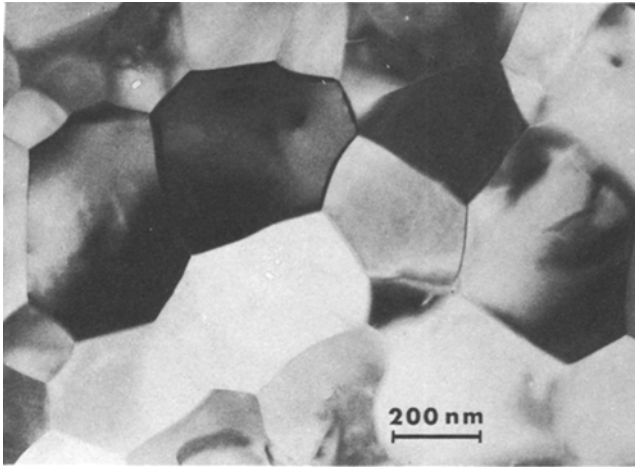


Figure 5 Laboratory silicon nitride microstructure.

of intergranular phase for Sample A. However, owing to the heterogeneous structure, it is not easy to get a quantitative distribution of the ICP. The exact determination of the nature of the ICP has been carried out by microdiffraction in the STEM mode (Fig. 10). The body-centred lattice and the value of the parameter $a = 1.227 \pm 0.010$ nm, obtained by using the Si_3N_4 matrix as a standard, indicate that the ICP is garnet-type. Moreover, quantitative X-ray microanalysis (Fig. 11) leads to the following composition: 6 Y, 4 Fe, 4 Si, $2/3$ Al. Since boron is not analysed but could be present in the garnet phase we tentatively propose the chemical formula $3 \text{Y}_2\text{O}_3$, 4FeO , 4SiO_2 , $1/3 \text{Al}_2\text{O}_3$, $2/3 \text{B}_2\text{O}_3$.

5.2.2. Characterization of a vitreous phase

Considering the similar granulometry of the

samples it was hoped to reveal a third phase which could be of prime significance for the mechanical behaviour. For this purpose selected area diffraction in TEM, microdiffraction in STEM and induced effects in TEM and STEM were combined.

In Sample B there was no evidence either from diffraction or microdiffraction of a third phase. On the other hand, while Sample A did not show a third phase from diffraction, a third glassy phase was found from microdiffraction. Thus it was inferred that there was a glassy phase at the garnet-matrix interface in Sample A: these results are corroborated by induced processes which do not show any glassy phase in Sample B but clearly indicate an interfacial glassy film between the matrix and the garnet phase at triple points (beam density 9 A cm^{-2}) (Fig. 12) and even continuously along the interfaces in Sample A (Fig. 13).

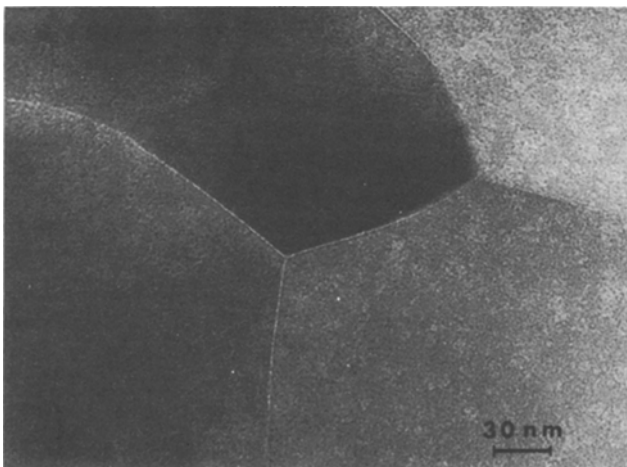


Figure 6 Laboratory silicon nitride: intergranular structure.

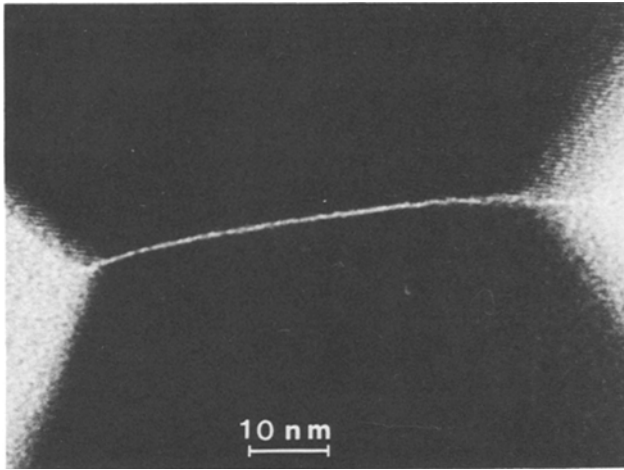


Figure 7 Laboratory silicon nitride: intergranular vitreous phase (IVP).

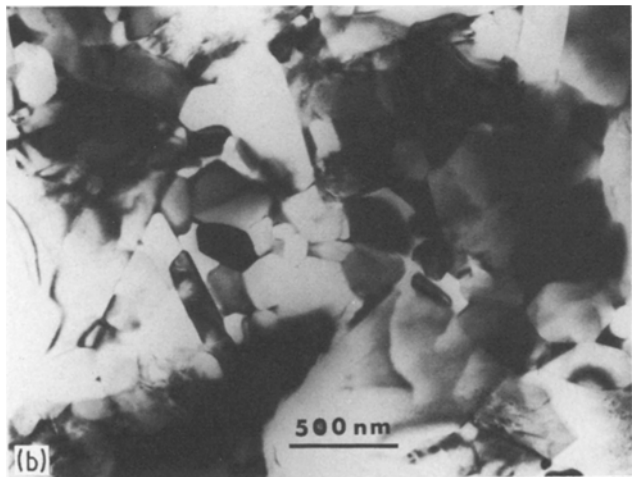
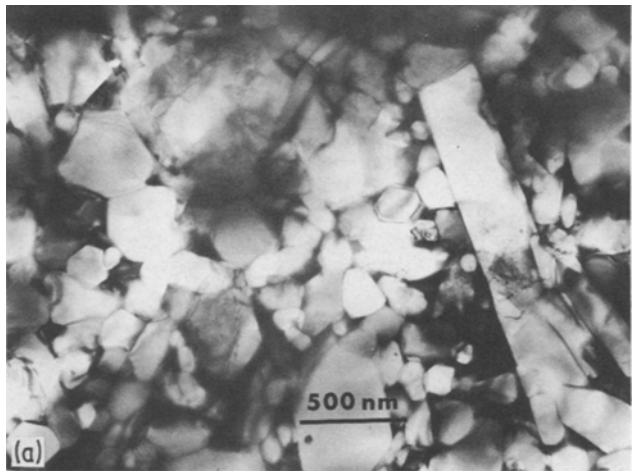


Figure 8 Microstructure of Sialons A and B (TEM).

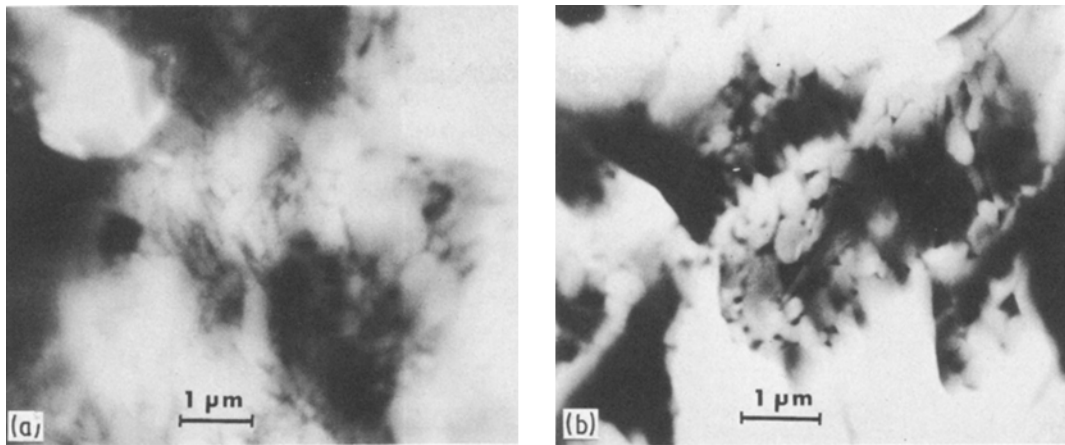


Figure 9 Microstructures of Sialons A and B (STEM).

6. Interpretation

The different intergranular structures of the nitrides studied correspond to four types illustrated in Fig. 14.

Let us now consider the high temperature strength and cutting efficiency of these materials according to their intergranular structure and try to explain the relationship between them.

6.1. High temperature mechanical strength

The existence of a thick intergranular phase, glassy or crystalline, will always be detrimental. For Type I structures (see Fig. 14) the softening of the glassy phase above 1100°C explains the strength drop-off of nitride at 1200°C . In the case of a thick crystalline second phase (Type 2), since there is no viscous flow available a brittle behaviour will control the strength degradation even at high temperatures.

In contrast the thin glassy film (Type 4), which is a very fine residue of a transient liquid phase [5] necessary for obtaining a highly dense and homogeneous nitride, will not diminish noticeably the strength which has been reported [10] to be almost constant up to 1400°C . It is also suggested that the conversion of α - to β - Si_3N_4 in this material could proceed through the diffusion of beryllium and oxygen in α - Si_3N_4 . This could explain the very fine grain sized microstructure – which is consistent with the retaining of strength at high temperature – contrary to what is observed in Type 1 where the said conversion leads to elongated β - Si_3N_4 grains resulting from a solution-precipitation process.

For Type 3 structures the exact role of the intermediate glassy film may be more difficult to elucidate since the strength decrease is stronger than for Type 2 structures, even below 1000°C .

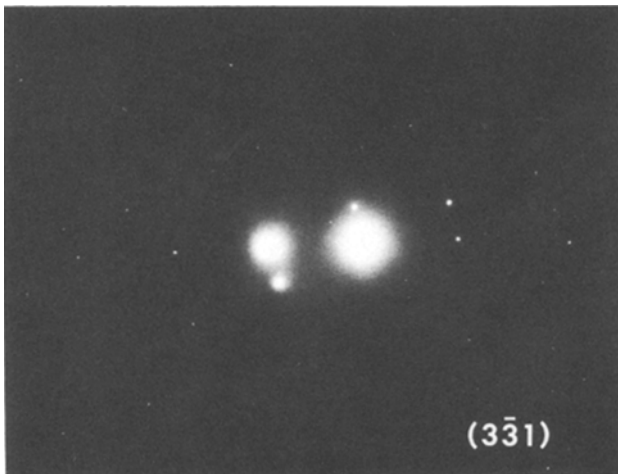


Figure 10 Microdiffraction on garnet phase.

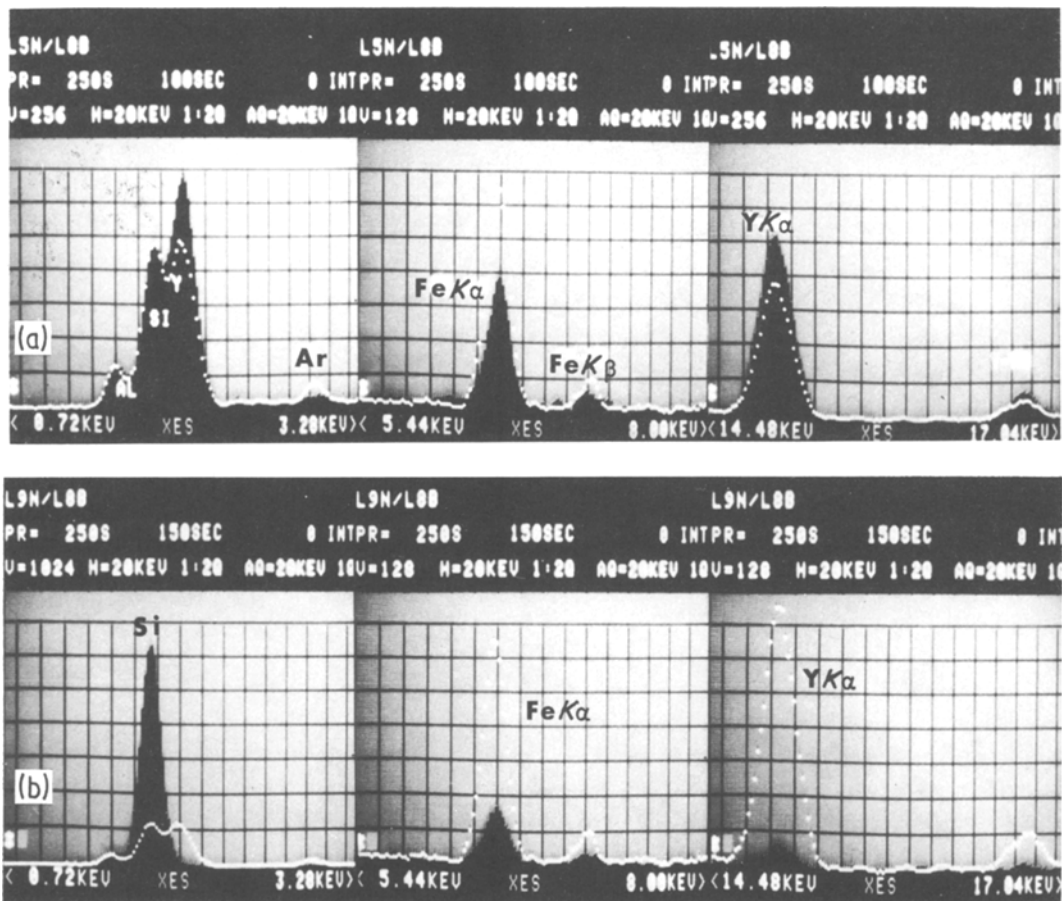


Figure 11 X-ray dispersive energy analysis on sialon phases. (a) Black, garnet; dotted line, glassy phase. (b) Black, β - Si_3N_4 ; dotted line, glassy phase.

This is undoubtedly related to the significant amount of impurities detected in Batch A sialon. Nevertheless above 1000°C alkaline and alkaline-earth elements such as sodium and calcium, which are known to enhance the steady-state creep rate [11], could act via the glassy intermediate film by lowering the viscosity or preventing its devitrification.

6.2. Cutting efficiency

The most interesting structures to compare here are Types 2 and 3. Type 2 will be characterized by an abrasive wear resulting from brittle failure of grains despite the high strength exhibited (toughness unchanged from room temperature). In contrast, the presence of the continuous glassy film at the garnet-nitride interface is likely to improve the cutting tool life by increasing the toughness on the one hand and by absorbing the stresses be-

tween two phases having different thermomechanical properties on the other hand [12, 13]. Thus this microstructure should be less sensitive to abrasive wear and to microcrack extension by accommodating stresses more easily.

Since the cutting tool temperature is likely to reach 1200°C in service, Type 1, which is characterized by a quick strength drop-off at 1000°C , will exhibit too small a viscosity at grain boundaries to prevent grain removal during metal machining.

The last type has not yet been tested for cutting application. Nevertheless, we can expect a fairly good behaviour from the very fine microstructure and the intergranular fracture mode exhibited. No commercial applications have been released to date for this beryllium-containing Si_3N_4 although there are some indications that cutting applications are being considered in Japan with this material.

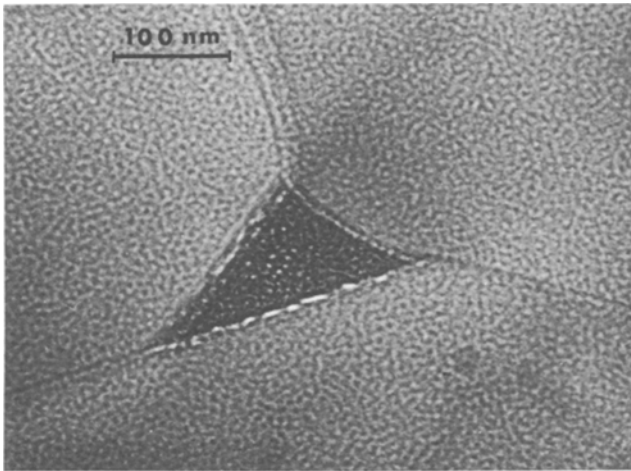


Figure 12 Intergranular structure of Sialon A as revealed by electron-induced processes (9 A cm^{-2}).

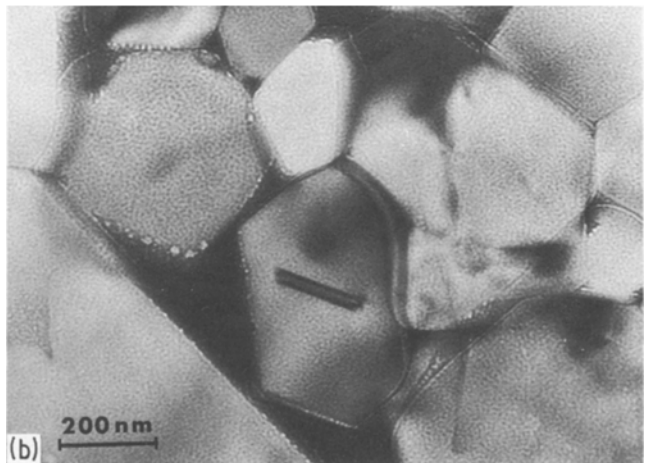
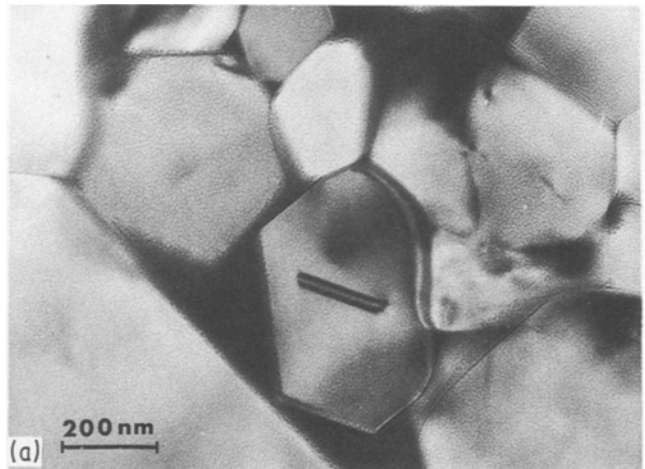


Figure 13 Continuous glassy film at the garnet-nitride interface. (a) Before irradiation; (b) after irradiation (9 A cm^{-2}).

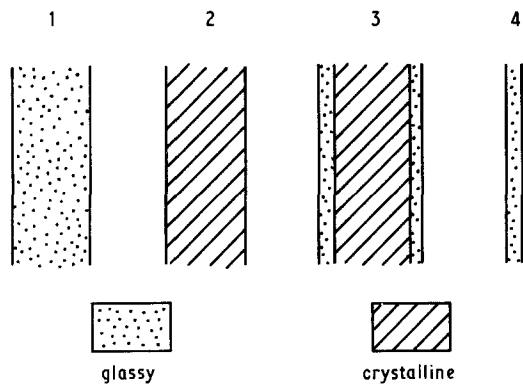


Figure 14 Intergranular structures of the substituted nitrides studied. 1. Thick vitreous second phase. 2. Thick crystalline second phase. 3. Thick crystalline second phase coupled with a vitreous film. 4. Vitreous film.

7. Conclusions

The microstructural analysis of several substituted nitrides has shown the outstanding influence of the intergranular structure on the mechanical strength. It appears that if an extended glassy intergranular phase is always detrimental for the properties, the existence of a very thin continuous glassy film may often be favourable and may be the best compromise available. In silicon nitride containing a small amount of beryllium and oxygen, this glassy film will be the only structure compatible with a dense and homogeneous material. In sialons, the presence of a glassy film

seems to confer a viscoplastic behaviour to the material at the cutting temperature. Thus the propagation of trans-granular and intergranular cracks is delayed and the tool life improved.

References

1. P. DREW and M. H. LEWIS, *J. Mater. Sci.* **9** (1974) 261.
2. J. Y. LAVAL and K. H. WESTMACOTT, *Inst. Phys. Conf. 52C* (1980) 295.
3. D. J. LAM, A. P. PAULIKAS and B. W. VEAL, *J. Non-Cryst. Solids* **42** (1980) 41.
4. M. PAULUS and F. REVERCHON, *J. Phys. et Rad. Suppl.* **6** (1961) 103A.
5. C. GRESKOVICH, *J. Mater. Sci.* **14** (1979) 2427.
6. K. H. JACK, *ibid.* **11** (1976) 1135.
7. J. Y. LAVAL, M. C. AMAMRA, D. BROUSSAUD and W. MUSTEL, *Rev. Chimie Minérale* **19** (1982) 690.
8. J. L. LINEWEAVER, *J. Appl. Phys.* **34** (1963) 1786.
9. J. Y. LAVAL, K. H. WESTMACOTT and M. C. AMAMRA, *J. de Phys.* **C9** (1982) 123.
10. T. A. PALM and C. D. GRESKOVICH, *Amer. Ceram. Bull.* **59** (1980) 447.
11. R. KOSSOWSKY, "Ceramics for High-performance Applications", edited by J. J. Burke, A. E. Gorum and R. N. Katz (Brook Hill Publ., Chestnut Hill, MA, 1974) pp. 347-71.
12. J. L. CHERMANT, M. MOUSSA and F. OSTERSTVEK, *Rev. Int. Hautes Temp. Réfract.* **18** (1981) 5.
13. A. E. PALADINO and E. A. MAJURRE, *J. Amer. Ceram. Soc.* **53** (1970) 98.

Received 22 March 1983
and accepted 23 January 1984